Chaotic Response and Bifurcation Analysis of Gear-Bearing System with and without Porous Effect under Nonlinear Suspension

Cai-Wan Chang-Jian

Abstract—This study presents a systematic analysis of the dynamic behaviors of a gear-bearing system with porous squeeze film damper (PSFD) under nonlinear suspension, nonlinear oil-film force and nonlinear gear meshing force effect. It can be found that the system exhibits very rich forms of sub-harmonic and even the chaotic vibrations. The bifurcation diagrams also reveal that greater values of permeability may not only improve non-periodic motions effectively, but also suppress dynamic amplitudes of the system. Therefore, porous effect plays an important role to improve dynamic stability of gear-bearing systems or other mechanical systems. The results presented in this study provide some useful insights into the design and development of a gear-bearing system for rotating machinery that operates in highly rotational speed and highly nonlinear regimes.

Keywords—Gear, PSFD, bifurcation, chaos.

I. INTRODUCTION

THE dynamic analysis of gears are presented in the past years. Many studies have focused on analyzing dynamic behaviors or performance of gears. Ozguven and Houser [1], [2] performed dynamic analysis on gears with the effects of variable mesh stiffness, damping, gear errors profile modification and backlash. Cai and Hayashi [3] calculated the optimum profile modification to obtain a zero vibration of the gear pair. Umezawa et al. [4] analyzed a single DOF numerical gear pair model and compared their numerical results with experimental dynamic transmission errors. Litvin, et al. [5] proposed a modified geometry of an asymmetric spur gear drive designed as a favorable shape of transmission errors of reduced magnitude and also reduced contact and bending stresses for an asymmetric spur gear drive. Guan, et al. [6] performed finite element method to simulate the geared rotor system constructed from beam and lumped mass/stiffness elements and compared the required actuation effort, control robustness and implementation cost. Giagopulos, et al. [7] presented an analysis on the nonlinear dynamics of a gear-pair system supported on rolling element bearings and used a suitable genetic algorithm to measure noise and model error. Theodossiades and Natsiavas [8] investigated dynamic responses and stability characteristics of rotordynamic systems interconnected with gear pairs and supported on oil journal

bearings. They found many non-periodic dynamic behaviors. They [9] also analyzed the motor-driven gear-pair systems with backlash and found periodic and chaotic dynamics in this system.

The current study performs a nonlinear analysis of the dynamic behavior of a gear pair system equipped with journal bearings and porous squeeze film damper under strongly nonlinear gear meshing force effect and nonlinear suspension effect. The discussions of dynamic behaviors of gear-bearing systems with and without porous effect are also provided. The non-dimensional equation of the gear-bearing system is then solved using the Runge-Kutta method. The non-periodic behavior of this system is characterized using phase diagrams, power spectra, Poincaré maps, bifurcation diagrams, Lyapunov exponents and the fractal dimension of the system. (with "Float over text" unchecked).

II. MATHEMATICAL MODEL

The model discussed in this study is the porous squeeze film damper mounted on a gear-bearing system with assumptions of nonlinear suspension, short journal bearing, strongly nonlinear gear meshing force and strongly nonlinear fluid film force effect, the cross section of the porous film and a schematic illustration of the dynamic model considered between gear and pinion as shown in Fig. 1. $O_g(X_g, Y_g)$ and $O_p(X_p, Y_p)$ are the gravity centers of the gear and pinion, respectively. $O_1 (X_1, Y_1)$ and $O_2(X_2, Y_2)$ are the geometric centers of the bearing 1 and bearing 2, respectively. $O_{j1}(X_{j1}, Y_{j1})$ and $O_{j2}(X_{j2}, Y_{j2})$ are the geometric centers of the journal 1 and journal 2, respectively. m_1 is the mass of the bearing housing for bearing 1 and m_2 is the mass of the bearing housing for bearing 2. m_p is the mass of the pinion and m_g is the mass of the gear. K_{p1} and K_{p2} are the stiffness coefficients of the shafts. K_{11}, K_{12}, K_{21} and K_{22} are the stiffness coefficients of the springs supporting the two bearing housings for bearing 1 and bearing 2. C_1 and C_2 are the damping coefficients of the supported structure for bearing 1 and bearing 2, respectively. K is the stiffness coefficient of the gear mesh. C is the damping coefficient of the gear mesh, e is the static transmission error and varies as a function of time. Note that (X_i, Y_i) are fixed coordinates, while (e_i, φ_i) are rotational coordinates, in which e_i is the offset of the journal center and φ_i is the attitude angle of the rotor relative to the X-coordinate direction.

Cai-Wan Chang-Jian is with the Department of Mechanical and Automation Engineering, I-Shou University, 1, Section 1, Hsueh-Cheng Rd., Ta-Hsu District, Kaohsiung City, Taiwan 84001, R.O.C. (e-mail: cwchangjian@ mail.isu.edu.tw).

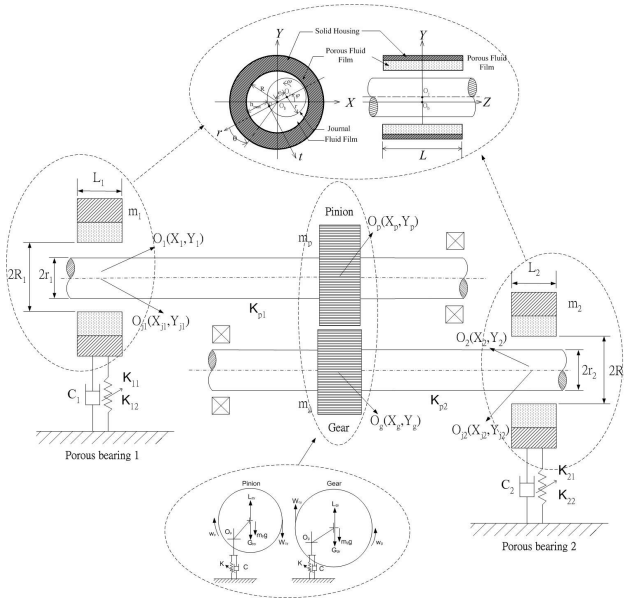## A. Principles of Force Equilibrium

Fig. 1 Schematic illustration of the gear-bearing system with PSFD, model of force diagram for pinion and gear, and cross section of the porous film

According to the principles of force equilibrium, the forces acting at the center of journal 1, i.e. O_{j1} (X_{j1}, Y_{j1}) and center of journal 2, i.e. O_{j2} (X_{j2}, Y_{j2}) are given by

$$F_{x1} = f_{e1}\cos\varphi_1 + f_{\varphi1}\sin\varphi_1 = K(X_p - X_{j1})/2 \qquad (1)$$

$$F_{y1} = f_{e1}\sin\varphi_1 - f_{\varphi1}\cos\varphi_1 = K(Y_p - Y_{j1})/2 \qquad (2)$$

$$F_{x2} = f_{e2}\cos\varphi_2 + f_{\varphi2}\sin\varphi_2 = K(X_g - X_{j2})/2 \qquad (3)$$

$$F_{y2} = f_{e2}\sin\varphi_2 - f_{\varphi2}\cos\varphi_2 = K(Y_g - Y_{j2})/2 \qquad (4)$$

in which f_{e1} and $f_{\varphi1}$ are the viscous damping forces in the radial and tangential directions for the center of journal 1, respectively, and f_{e2} and $f_{\varphi2}$ are the viscous damping forces in the radial and tangential directions for the center of journal 2, respectively.

B. Nonlinear Fluid Film Force

In this study, the modified Reynolds equation and the short bearing assumption ($\frac{L}{D} < 0.25$、 $\frac{\partial p}{\partial \theta} << \frac{\partial p}{\partial z}$) is used.

$$\frac{\partial}{\partial z}(12\Phi H \frac{\partial p}{\partial z}) = 6\mu U \frac{\partial h}{\partial x} + 12\mu \frac{\partial h}{\partial t} \qquad (5)$$

where Φ is permeability of porous ring, Φ can also be performed as $\Phi = \frac{Q\mu H}{\Delta p A}$, A is area of porous ring, H is film thickness of porous ring, Δp is pressure difference of porous ring, $\frac{\partial h}{\partial x} = -\frac{c\varepsilon}{R}\sin\theta$, $\frac{\partial h}{\partial t} = c\dot{\varepsilon}\cos\theta + c\varepsilon\dot{\varphi}\sin\theta$, $x = R\theta$, $U = R\omega$,

$\varepsilon = \frac{e}{c}$ and $h = c(1 + \varepsilon\cos(\gamma - \varphi(t))) = c(1 + \varepsilon\cos\theta)$. Then Reynolds equation can be rewritten as

$$\frac{\partial^2 p}{\partial z^2} = \frac{-6\mu\omega c\varepsilon\sin\theta + 12\mu(c\dot{\varepsilon}\cos\theta + c\varepsilon\dot{\varphi}\sin\theta)}{12\Phi H} \qquad (6)$$

with boundary conditions $\begin{cases} \frac{\partial p}{\partial z} = 0, & z = 0 \\ p = 0, & z = \pm\frac{L}{2} \end{cases}$

then

$$p = -\frac{3\mu c}{12\Phi H}[(\omega - 2\dot{\varphi})\varepsilon\sin\theta - 2\dot{\varepsilon}\cos\theta](z^2 - \frac{L^2}{4}) \qquad (7)$$

The resulting damping forces about the journal center in the radial and tangential directions are determined by integrating (7) over the area of the journal sleeve on the basis of the hypothesis of cavitating conditions with π-film.

$$f_r = \int_0^\pi \int_{-\frac{L}{2}}^{\frac{L}{2}} p(\theta, z)R\cos\theta\, dz\, d\theta \qquad (8)$$

$$f_t = \int_0^\pi \int_{-\frac{L}{2}}^{\frac{L}{2}} p(\theta, z)R\sin\theta\, dz\, d\theta \qquad (9)$$

Let $\psi = \frac{12\Phi H}{c^3}$, $f_e = -f_r$, $f_\varphi = -f_t$

$$f_e = -\frac{\mu L^3 R}{2c^2\psi}\int_0^\pi \{[(\omega - 2\dot{\varphi})\varepsilon\sin\theta - 2\dot{\varepsilon}\cos\theta]\sin\theta\} d\theta \qquad (10)$$

$$f_\varphi = -\frac{\mu L^3 R}{2c^2\psi}\int_0^\pi \{[(\omega - 2\dot{\varphi})\varepsilon\sin\theta - 2\dot{\varepsilon}\cos\theta]\sin\theta\} d\theta \qquad (11)$$

Substituting (10) and (11) into (1), (2), (3) and (4), respectively, enables the values of F_{x1}, F_{x2}, F_{y1} and F_{y2} to be obtained.

C. Equations of Motion

The differential equations of motion used to describe geometric centers of gear and pinion $(O_g(X_g, Y_g)$ and $O_p(X_p, Y_p))$ can be written as

$$m_p\ddot{X}_p + C\dot{X}_p + KX_p = W_{cx} + F_{x1} + KX_{p0} \qquad (12)$$

$$m_p\ddot{Y}_p + C\dot{Y}_p + KY_p = L_{py} - G_{py} - W_{cy} - m_p g + F_{y1} + KY_{p0} \qquad (13)$$

$$m_g\ddot{X}_g + C\dot{X}_g + KX_g = -W_{cx} - F_{x2} + KX_{g0} \qquad (14)$$

$$m_g\ddot{Y}_g + C\dot{Y}_g + KY_g = L_{py} - G_{py} + W_{cy} - m_g g + F_{y2} + KY_{g0} \qquad (15)$$

where L_{py} and L_{gy} are the centrifugal forces in the vertical gear mesh direction for pinion and gear, G_{py} and G_{gy} are the inertia forces in the vertical gear mesh direction for pinion and gear, W_{cx} is the dynamic gear mesh force in the horizontal direction, and W_{cy} is the dynamic gear mesh force in the vertical direction. L_{py}, L_{gy}, G_{py}, G_{gy}, W_{cx} and W_{cy} can be performed as

$$L_{py} = m_p e_p \omega_p^2 \sin\theta_1 \qquad (16)$$

$$L_{gy} = m_g e_g \omega_g^2 \sin\theta_2 \qquad (17)$$

$$G_{py} = m_p e_p \ddot{\theta}_1 \cos\theta_1 \qquad (18)$$

$$G_{gy} = m_g e_g \ddot{\theta}_2 \cos\theta_2 \qquad (19)$$

$$W_{cx} = C_m(\dot{X}_p - \dot{X}_g - e_p\Omega\sin(\Omega t)) + K_m(X_p - X_g - e_p\cos(\Omega t)) \qquad (20)$$

$$W_{cy} = C_m(\dot{Y}_p - \dot{Y}_g - e_p\Omega\cos(\Omega t)) + K_m(Y_p - Y_g - e_p\sin(\Omega t)) \qquad (21)$$

Substituting (16) to (21) into (12) to (15), yields the following equations:

$$m_p\ddot{X}_p + C\dot{X}_p + KX_p = C_m(\dot{X}_p - \dot{X}_g - e_p\Omega\sin(\Omega t)) \\ + K_m(X_p - X_g - e_p\cos(\Omega t)) + F_{x1} + KX_{p0} \qquad (22)$$

$$m_p\ddot{Y}_p + C\dot{Y}_p + KY_p = m_p e_p\omega_p^2\sin\theta_1 - \\ C_m(\dot{Y}_p - \dot{Y}_g - e_p\Omega\cos(\Omega t)) - \\ K_m(Y_p - Y_g - e_p\sin(\Omega t)) - m_p g + F_{y1} + KY_{p0} \qquad (23)$$

$$m_g\ddot{X}_g + C\dot{X}_g + KX_g = -C_m(\dot{X}_p - \dot{X}_g - e_p\Omega\sin(\Omega t)) \\ - K_m(X_p - X_g - e_p\cos(\Omega t)) + F_{x2} + KX_{g0} \qquad (24)$$

$$m_g\ddot{Y}_g + C\dot{Y}_g + KY_g = m_g e_g\omega_g^2\sin\theta_2 \\ - C_m(\dot{Y}_p - \dot{Y}_g - e_p\Omega\cos(\Omega t)) \\ + K_m(Y_p - Y_g - e_p\sin(\Omega t)) - m_g g + F_{y2} + KY_{g0} \qquad (25)$$

The equations of motion of the center of bearing 1 (X_1, Y_1) and the center of bearing 2 (X_2, Y_2) under the assumption of nonlinear suspension can be written as

$$m_1\ddot{X}_1 + c_1\dot{X}_1 + k_{11}X_1 + k_{12}X_1^3 = F_{x1} \qquad (26)$$

$$m_1\ddot{Y}_1 + c_1\dot{Y}_1 + k_{11}Y_1 + k_{12}Y_1^3 = -m_1 g + F_{y1} \qquad (27)$$

$$m_2\ddot{X}_2 + c_2\dot{X}_2 + k_{21}X_2 + k_{22}X_2^3 = F_{x2} \qquad (28)$$

$$m_2\ddot{Y}_2 + c_2\dot{Y}_2 + k_{21}Y_2 + k_{22}Y_2^3 = -m_2 g + F_{y2} \qquad (29)$$

D. Dimensionless of Dynamic Equations of Motion

Equations (21)-(24) and (25)-(28) can be expressed as

$$\varepsilon_1' = \frac{\beta_1 c K_p[(y_p - y_1 - \varepsilon_1\sin\varphi_1)\cos\varphi_1 - (x_p - x_1 - \varepsilon_1\cos\varphi_1)\sin\varphi_1]}{4\alpha_1(\gamma_1\delta_1 - \beta_1^2)\omega} \\ - \frac{\delta_1 c K_p[(x_p - x_1 - \varepsilon_1\cos\varphi_1)\cos\varphi_1 + (y_p - y_1 - \varepsilon_1\sin\varphi_1)\sin\varphi_1]}{4\alpha_1(\gamma_1\delta_1 - \beta_1^2)\omega} \qquad (30)$$

$$\varphi_1' = \frac{1}{2} - \frac{c K_p[(y_p - y_1 - \varepsilon_1\sin\varphi_1)\cos\varphi_1 - (x_p - x_1 - \varepsilon_1\cos\varphi_1)\sin\varphi_1]}{4\alpha_1\delta_1\varepsilon_1\omega} \\ - \frac{\beta_1^2 c K_p[(y_p - y_1 - \varepsilon_1\sin\varphi_1)\cos\varphi_1 - (x_p - x_1 - \varepsilon_1\cos\varphi_1)\sin\varphi_1]}{4\alpha_1\varepsilon_1\delta_1(\gamma_1\delta_1 - \beta_1^2)\omega} \\ + \frac{\beta_1^2 c K_p[(y_p - y_1 - \varepsilon_1\sin\varphi_1)\cos\varphi_1 + (x_p - x_1 - \varepsilon_1\cos\varphi_1)\sin\varphi_1]}{4\alpha_1\varepsilon_1\delta_1(\gamma_1\delta_1 - \beta_1^2)\omega} \qquad (31)$$

$$\varepsilon_2' = \frac{\beta_1 c K_p[(y_g - y_2 - \varepsilon_2\sin\varphi_2)\cos\varphi_2 - (x_g - x_2 - \varepsilon_2\cos\varphi_2)\sin\varphi_2]}{4\alpha_1(\gamma_1\delta_1 - \beta_1^2)\omega} \\ - \frac{\delta_1 c K_p[(x_g - x_2 - \varepsilon_2\cos\varphi_2)\cos\varphi_2 + (y_g - y_2 - \varepsilon_2\sin\varphi_2)\sin\varphi_2]}{4\alpha_1(\gamma_1\delta_1 - \beta_1^2)\omega} \qquad (32)$$

$$\varphi_2' = \frac{1}{2} - \frac{c K_p[(y_g - y_2 - \varepsilon_2\sin\varphi_2)\cos\varphi_2 - (x_g - x_2 - \varepsilon_2\cos\varphi_2)\sin\varphi_2]}{4\alpha_1\delta_1\varepsilon_2\omega} \\ + \frac{\beta_1^2 c K_p[(y_g - y_2 - \varepsilon_2\sin\varphi_2)\cos\varphi_2 + (x_g - x_2 - \varepsilon_2\cos\varphi_2)\sin\varphi_2]}{4\alpha_1\varepsilon_2\delta_1(\gamma_1\delta_1 - \beta_1^2)\omega} \\ - \frac{\beta_1\delta_1 c K_p[(x_g - x_2 - \varepsilon_2\cos\varphi_2)\cos\varphi_2 + (y_g - y_2 - \varepsilon_2\sin\varphi_2)\sin\varphi_2]}{4\alpha_1\varepsilon_2\delta_1(\gamma_1\delta_1 - \beta_1^2)\omega} \qquad (33)$$

$$x_p'' = -\frac{2\xi_2}{s}x_p' - \frac{1}{s^2}\left(x_p - x_1 - \varepsilon_1\cos\varphi_1\right) + \beta\cos(\phi/4) \\ - \frac{2\xi_3}{s}(x_p' - x_g' - E_p\sin\phi) - \frac{\Lambda}{s^2}(x_p - x_g - E_p\cos\phi) \qquad (34)$$

$$y_p'' = -\frac{2\xi_2}{s}y_p' - \frac{1}{s^2}\left(y_p - y_1 - \varepsilon_1\sin\varphi_1\right) + \beta\sin(\phi/4) - \frac{f}{s^2} \\ - \frac{2\xi_3}{s}(y_p' - y_g' - E_p\cos\phi) - \frac{\Lambda}{s^2}(y_p - y_g - E_p\sin\phi) \qquad (35)$$

$$x_g'' = -\frac{2\xi_4}{s}x_g' - \frac{1}{s^2}\left(x_g - x_2 - \varepsilon_2\cos\varphi_2\right) + \beta_g\cos(\phi/8) + \\ \frac{2\xi_5}{s}(x_p' - x_g' - E_p\sin\phi) - \frac{\Lambda_g}{s^2}(x_p - x_g - E_p\cos\phi) \qquad (36)$$

$$y_g'' = -\frac{2\xi_4}{s}y_g' - \frac{1}{s^2}\left(y_g - y_2 - \varepsilon_2\sin\varphi_2\right) + \beta_g\sin(\phi/8) \\ + \frac{2\xi_5}{s}(y_p' - y_g' - E_p\cos\phi) + \frac{\Lambda_g}{s^2}(y_p - y_g - E_p\sin\phi) - \frac{f_g}{s^2} \qquad (37)$$

$$x_1'' + \frac{2\xi_1}{s_1}x_1' + \frac{1}{s_1^2}x_1 + \frac{\alpha_1}{s^2}x_1^3 - \frac{1}{2C_{1p}s^2}(x_p - x_1 - \varepsilon_1\cos\varphi_1) = 0 \qquad (38)$$

$$y_1'' + \frac{2\xi_1}{s_1}y_1' + \frac{1}{s_1^2}y_1 + \frac{\alpha_1}{s^2}y_1^3 - \frac{1}{2C_{om}s^2}(y_p - y_1 - \varepsilon_1\sin\varphi_1) + \frac{f}{s^2} = 0 \qquad (39)$$

$$x_2'' + \frac{2\xi_6}{s_2}x_2' + \frac{1}{s_2^2}x_2 + \frac{\alpha_2}{s^2}x_2^3 - \frac{1}{2C_{2p}s^2}(x_g - x_2 - \varepsilon_2\cos\varphi_2) = 0 \qquad (40)$$

$$y_2'' + \frac{2\xi_6}{s_2}y_2' + \frac{1}{s_2^2}y_2 + \frac{\alpha_2}{s^2}y_2^3 - \frac{1}{2C_{2p}s^2}(y_g - y_2 - \varepsilon_2\sin\varphi_2) + \frac{f}{s^2} = 0 \qquad (41)$$

where $\quad \alpha_1 = -\dfrac{\mu L^3 R}{2c^2\psi}$, $\quad \beta_1 = \int_0^\pi \sin\theta\cos\theta d\theta$, $\quad \gamma_1 = \int_0^\pi \cos\theta\cos\theta d\theta$,

$\delta_1 = \int_0^\pi \sin\theta\sin\theta d\theta$

Equations (30)-(41) describe a non-linear dynamic system. In the current study, the approximate solutions of these coupled non-linear differential equations are obtained using the fourth order Runge-Kutta numerical scheme.

III. NUMERICAL RESULTS AND DISCUSSIONS

In the present study, the nonlinear dynamics of the gear-bearing system shown in Fig. 1 are analyzed using Poincaré maps, bifurcation diagrams, the Lyapunov exponent and the fractal dimension. A number of parameters can be used to generate bifurcation diagrams, e.g. the rotating speed, unbalance, damping coefficient, stiffness coefficient, etc. In practical bearing systems, the rotational speed ratio s is commonly used as a significant control parameter. Accordingly, the dynamic behavior of the current gear-bearing system with and without porous effect (ψ =0.0 for the case without porous effect , ψ =0.0001, 0.001 and 0.1 for the cases with porous effect) was examined using the dimensionless rotational speed ratio s as a bifurcation control parameter. Fig. 2 presents the bifurcation characteristics of the pinion center and bearing center displacement in the vertical direction against the dimensionless rotational speed ratio, s with ψ =0.0. It can be seen that the motion is non-periodic at almost all rotating speeds. We also find that dynamic behaviors with ψ =0.0 (zero permeability or the case without porous effect) are almost non-periodic and the dynamic amplitudes become greater and greater with increasing rotational speed ratios. In order to explore different bifurcation phenomena and dynamic behaviors, other permeability is also taken into consideration.
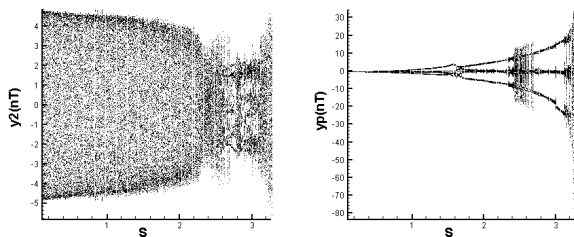

Fig. 2 Bifurcation diagrams of gear center using dimensionless rotational speed ratio, s, as bifurcation parameter (ψ =0.0)
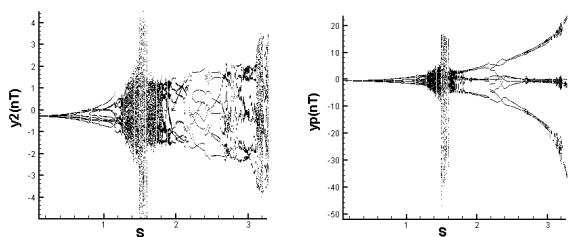

Fig. 3 Bifurcation diagrams of gear center using dimensionless rotational speed ratio, s, as bifurcation parameter (ψ =0.0001)
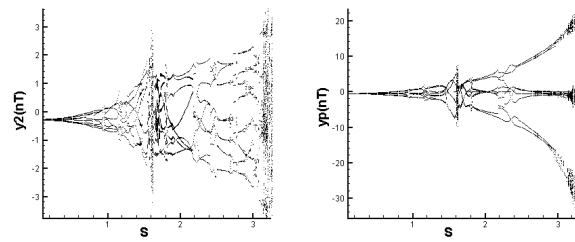

Fig. 4 Bifurcation diagrams of gear center using dimensionless rotational speed ratio, s, as bifurcation parameter (ψ =0.001)
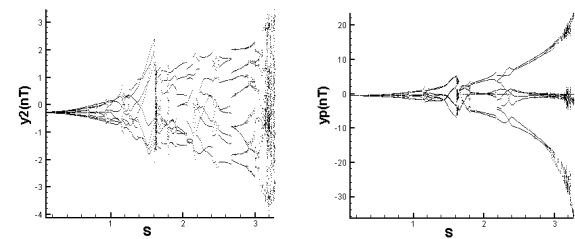

Fig. 5 Bifurcation diagrams of gear center using dimensionless rotational speed ratio, s, as bifurcation parameter (ψ =0.1).

Fig. 3 shows the bifurcation diagrams with ψ =0.0001. The bifurcation diagrams show that at low rotating speeds the dynamic motion is sub-harmonic with period 8. At about s>1.18 the motions becomes chaotic. The chaotic state remains for a short range of rotating speed ratios (1.18<s<1.80). At around s=1.48~1.60, chaotic vibration also behaves highly amplitude and then the motion becomes 8T periodic motion at s=1.61~3.10. Finally, at s=3.11 it again becomes chaotic vibration. Fig. 4 is the bifurcation diagram with ψ =0.001 and chaotic motions are found at s=1.60~1.62 and s>3.15. It performs sub-harmonic motions with period 8 at almost all another rotating speed ratios. With greater permeability for ψ =0.1 as shown in Fig. 5 show that the vibration behaves 8T periodic motions for almost all the rotating speeds except at s=1.60~1.62 and s>3.15. We will not be able to distinguish dynamic behaviors to be chaotic or quasi-periodic motions only by dynamic orbits or bifurcation diagrams, but also use other schemes such as Poincaré maps, Lyapunov exponent or fractal dimension to specify our dynamic responses. Thus we introduce Figs. 6 and 7, i.e. phase diagram, power spectrum, Poincaré Map, Lyapunov exponent and fractal dimension for y_2 and y_p with $s=3.27$, and we can find the simulation results are corresponding with one another. Phase diagrams show disordered dynamic behaviors; power spectra reveal numerous excitation frequencies; the return points in the Poincaré maps form geometrically fractal structures; the maximum Lyapunov exponent is positive; the fractal dimensions are found to be 1.28 for y_p and 1.41 for y_2.
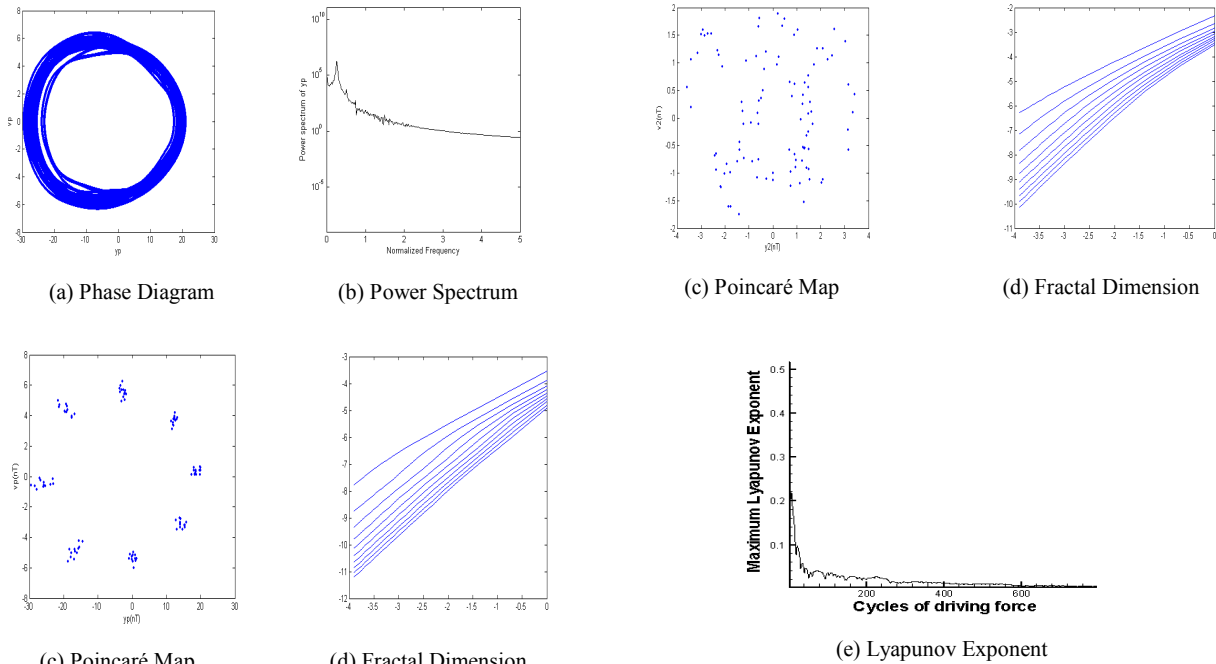
(a) Phase Diagram

(b) Power Spectrum

(c) Poincaré Map

(d) Fractal Dimension

(c) Poincaré Map

(d) Fractal Dimension

(e) Lyapunov Exponent

Fig. 7 Simulation results obtained for gear-bearing system with s=3.27 (y_2)

(e) Lyapunov Exponent

Fig.6 Simulation results obtained for gear-bearing system with s=3.27 (y_p)

(a) Phase Diagram

(b) Power Spectrum

IV. CONCLUSIONS

Effects of change in the rotating speed ratio on the vibration features of the gear-bearing system are investigated theoretically in this paper. It can be seen that the system exhibits very rich forms of nT-periodic and chaotic vibrations. The bifurcation diagrams also reveal that greater values of permeability may not only improve non-periodic motions effectively, but also suppress dynamic amplitudes. Therefore, we may conclude that porous effect can improve dynamic stability of gear-bearing systems. Overall, the results presented in this study provide a detailed understanding of the nonlinear dynamic response of a gear-bearing system under typical rotational speed conditions. Specifically, the results enable suitable values of the rotational speed ratios to be specified such that chaotic behavior can be avoided, thus reducing the amplitude of the vibration within the system and extending the system life.

REFERENCES

[1] H.N. Ozguven, and D.R. Houser, "Mathematical models used in gear dynamics," *J. Sound Vib.* vol. 121, 1988, pp. 383-411.

[2] H.N. Ozguven, and D.R. Houser, "Dynamic analysis of high speed gears by using loaded static transmission error," *J. Sound Vib.* vol. 125, 1988, pp. 71-83.

[3] Y. Cai, and T. Hayashi, "The linear approximated equation of vibration of a pair of spur gears," *ASME J. Mech. Trans. Auto. Design* vol. 116, 1994,
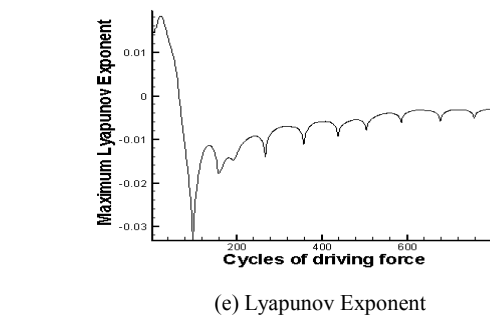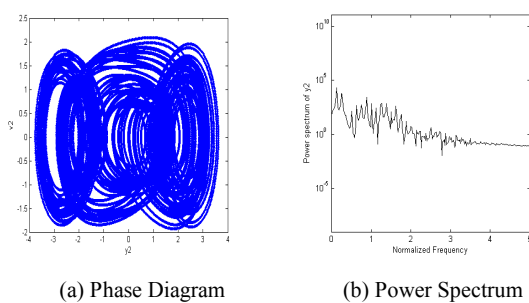
pp. 558-564.

[4] K. Umezawa, and T. Sato, "Simulation on rotational vibration of spur gears," *Bull. Jpn. So. Mech. Eng.* vol. 27, 1984, pp. 102-109.

[5] L. Litvin, Q. Lian, and A.L. Kapelevich, "Asymmetric modified spur gear drives: reduction of noise, localization of contact, simulation of meshing and stress analysis," *Comput. Meth. Appl. Mech. Eng.* vol. 188, 2000, pp. 363-390.

[6] Y.H. Guan, M.F. Li, T.C. Lim, and W.S. Shepard, "Comparative analysis of actuator concepts for active gear pair vibration control," *J. Sound Vib.* vol. 269, 2004, pp. 273-294.

[7] D. Giagopulos, C. Salpistis, and S. Natsiavas, "Effect of non-linearities in the identification and fault detection of gear-pair systems," *Int. J. Nonlinear Mech.* vol. 41, 2006, pp. 213-230.

[8] S. Theodossiades, and S. Natsiavas, "On geared rotordynamic systems with oil journal bearings," *J. Sound Vib.* vol. 243(4), 2001, pp. 721-745.

[9] S. Theodossiades, and S. Natsiavas, "Periodic and chaotic dynamics of motor-driven gear-pair systems with backlash," *Chaos Solitons Fractals* vol. 12, 2001, pp. 2427-2440.

Cai-Wan Chang-Jian was born in Kaohsiung City, Taiwan in 1977. He got his BSc degree from Department of Mechanical Engineering, Yuan Ze University, Taiwan, in 1999. He then obtained his MSc and PhD degree from National Cheng-Kung University (Taiwan), in 2001 and 2006, respectively.

He is currently an associate professor at the Department of Mechanical and Automation Engineering, I-Shou University, Taiwan. His majors are control system, nonlinear dynamic analysis and dynamical system analysis. He is the author and co-author for more than fifty research journal paper. His recent research includes nonlinear dynamics and control, measurement of thermal deformation, fuel cell and finite element analysis.

Assoc. Prof. Chang-Jian is also an editor of Journal of the Chinese Society of Mechanical Engineers and International Journal of Control Engineering and Technology.